

Method for enlarging the dynamic aperture of accelerator lattices

Weishi Wan* and John R. Cary

Center for Integrated Plasma Studies and Department of Physics, University of Colorado, Boulder, Colorado 80309-0390
(Received 27 July 1999; revised manuscript received 30 May 2001; published 20 August 2001)

A method for finding four-dimensional symplectic maps with an enlarged nearly integrable region is described. The method relies on solving for parameter values at which the linear stability factors of the fixed points (periodic orbits) of the map have the values corresponding to integer island tunes. This method is applied to accelerator lattices in order to increase dynamic aperture. The result shows a significant increase of the dynamic aperture after correction.

DOI: 10.1103/PhysRevSTAB.4.084001

PACS numbers: 29.27.-a, 41.85.Ja, 47.20.Ky

I. INTRODUCTION

Much progress has been made in the problem of determining whether a dynamical system is chaotic or stable in a finite phase space region. Poincaré [1] showed that, for a general perturbation of an integrable multidimensional oscillator, there is no invariant analytic in the perturbation parameter. The problem of small denominators in normal form theory [2] prevents one from finding a convergent invariant in the neighborhood of a linearly stable fixed point. The understanding of what happens when an integrable system is perturbed was greatly increased by the Kol'mogorov-Arnold-Moser (KAM) theorem [3–6] which showed that some invariant surfaces remain (provided that the linear frequencies in normal form theory are not linearly related with integers smaller than 4). Complementarily, Melnikov [7] and subsequent work [8] on the intersection of stable and unstable manifold showed that chaotic motion is very easy to find. These advances helped greatly to determine the stability of a given Hamiltonian system, such as the motion of the asteroids or the stability of the solar system.

In contrast, there is another class of problems in which one has freedom in choosing the Hamiltonian, and, for various reasons, one would like to have a system that is either completely chaotic or uniformly integrable. For example, one might desire a chaotic fluid flow so that chemicals are mixed uniformly in a short time. An example of needing integrability occurs in the design of systems that must confine particles, such as fusion confinement devices or particle accelerators. The goal of this paper is to outline in detail a method which allows one to find symplectic maps with increased stable region and present an accelerator lattice which shows a significant increase in dynamic aperture after the method is applied. Although the method is general, it is presented mostly in the context of its appli-

cation in circular particle accelerators. Following the tradition of the accelerator community, we define “dynamic aperture” as the equivalent radius of the area in the x - y plane such that all particles (with initial p_x and p_y zero) inside the circle defined by it are stable after a given number of turns. Generally, the dynamic aperture so defined scales as the fourth root of the well-confined phase space volume.

The restrictions that arise in real systems make this problem nontrivial. Without restrictions, one can write down any number of integrable Hamiltonians. The freedom of an accelerator designer, on the other hand, is limited by the fact that transverse confinement of particles in a circular accelerator is provided by various kinds of magnets, namely, dipoles, quadrupoles, sextupoles, and other multipoles. As a result, it has been difficult to increase dynamic aperture significantly, and there is sustained interest in the subject [9–44].

The sextupoles necessary in most accelerators, the large divergence of the beam in certain colliders [45] and the fringe field of large aperture accelerators with large physical aperture [46], make virtually every accelerator, in practice, intrinsically nonlinear. Magnet imperfections are an additional source of nonlinearity. Because additional effects, such as power supply ripple, scattering from residual gas molecules, and intrabeam scattering, generally reduce the dynamic aperture, it is desirable to have the nonlinearity determined dynamic aperture be as large as possible.

Previous approaches to increasing dynamic aperture were based on perturbation theory. (Ruggiero [47], for example, discusses the application of perturbation theory to the analysis of the beam-beam interaction.) Perturbation theoretic approaches work well when only a few low-order resonances dominate and the modifications to the lattice needed to increase the dynamic aperture are small. Our method, which is not based on perturbation theory, circumvents these limitations. Instead of focusing on the normal form representation of the resonance driving terms, our method utilizes the connection between island tunes and resonance strength, which remains valid even at large nonlinearity provided one is close to integrability

*Present address: Lawrence Berkeley National Laboratory, Berkeley, CA 94720.

(as is the case in the transition region near the dynamic aperture).

The basic idea of this new method [48] has been applied in the context of finding a three-dimensional toroidal magnetic field with lines lying on nested toroidal surfaces [49], which is a one and a half degrees of freedom Hamiltonian problem [50]. A series of designs found by using these ideas was published [51]. Subsequently, we successfully applied these ideas to the similar problem of the dynamics in the uncoupled horizontal dynamics of an accelerator lattice [52].

However, the dynamic aperture of the four-dimensional systems was found to have decreased. These results meant that to be able to increase dynamic aperture in Hamiltonian systems of two and a half degrees of freedom, one would have to consider the full dynamics. A method [53] was developed to do just that, and a brief presentation was published [54]. In this paper, we show in detail how this could be done. We begin, in the following section, by introducing the method from the analytic point of view. This is followed by an example demonstrating the application of the method to an accelerator lattice which shows a significant increase of the dynamic aperture. Implications of this method are discussed in the last section.

II. ANALYTICAL BACKGROUND AND DESCRIPTION OF THE METHOD

Our method for reducing chaotic motion and, therefore, increasing the dynamic aperture relies on the connection between the presence of resonances and the existence of chaotic motion. Thus, as we know from, e.g., Chirikov's analyses [55,56], the overlap of resonances leads to chaotic regions and, hence, a reduction of the dynamic aperture. Of course, one can have large resonances in nonlinear systems without chaotic motion, as in the Toda lattice [57]. Nevertheless, it remains true that the path to chaotic dynamics is through the growth of resonances. This leads us to propose a methodology: reduce the strengths of the resonances, as this will lead to a reduction of the chaotic region and a concomitant increase in the dynamic aperture. This is borne out by experience, which has shown that resonance correction and/or avoidance typically lead to increases in dynamic aperture.

There remains, then, the development of a convenient measurement of resonance strength. As typically introduced, resonances are found in perturbation theory—through the analysis of the motion near rational surfaces of an integrable Hamiltonian in the presence of a perturbation. However, perturbation results are not easily applied to chaotic regions, as there is no unique way to find the underlying integrable Hamiltonian and from that carry out the perturbation analysis. Indeed, in the strongly chaotic limit, resonancelike motion may not be observable. However, the fixed points associated with a resonance exist significantly after the resonance region is largely chaotic.

Furthermore, one can relate the matrix invariants of the symplectic matrix describing linearized motion near the fixed point to the strength of the associated nonlinear resonance. Thus, one can use these matrix invariants as a proxy for the resonance strengths. Per the comments of the previous paragraph, these matrix invariants can be found for fixed points in systems arbitrarily far from integrable.

The purpose of this section is to provide the basis of this understanding. We briefly discuss resonances and fixed points for perturbed four-dimensional maps. We show how the resonance strength is related to two parameters, A and B , which are invariants of the symplectic map associated with linearized motion near a fixed point. Next, we note that A and B have particular values (4 and 6) when there is no resonance. This leads us to propose increasing dynamic aperture by solving for values of parameters such that $A = 4$ and $B = 6$.

A. Resonances

Resonances arise in the perturbation of the Hamiltonian. To study them quantitatively, we Fourier expand the perturbing Hamiltonian in the angle variables and the periodic time.

$$H = H_0(\mathbf{J}) + \sum_{l,m} H_{1lm}(\mathbf{J}) \cos[l \cdot \theta - m\Omega s + \phi_{lm}(\mathbf{J})]. \quad (1)$$

Resonance occurs at the places where the phase is stationary when evolved according to the unperturbed Hamiltonian,

$$\begin{aligned} \left(\frac{d}{ds}\right)_0 (l_1\theta_1 + l_2\theta_2 - m\Omega s + \phi_{l_1l_2m}) \\ = l_1\omega_1(\mathbf{J}) + l_2\omega_2(\mathbf{J}) - m\Omega = 0. \end{aligned} \quad (2)$$

Thus, resonances correspond to curves in the action space, as sketched in Fig. 1. In terms of the tunes, this relation is

$$l_1\nu_1(\mathbf{J}) + l_2\nu_2(\mathbf{J}) - m = 0, \quad (3)$$

which means that resonance can certainly occur if the tunes are rational, but it can also occur if the tunes are irrational but the ratio is rational.

To put it loosely, the KAM theorem states that invariant tori of a given frequency pair may survive provided that the relations of the form (3) are difficult to satisfy. In essence, this means that the value of the left-hand side of Eq. (3) does not decrease too rapidly as larger integers are used. Unfortunately, the existence of invariant tori does not guarantee the absence of phase-space transport (i.e., emittance blowup in accelerators). Invariant tori are points in the action plane (see Fig. 1). Hence, in principle, a trajectory could access large values of the actions and, thus, the vacuum pipe in an accelerator by wandering around the KAM tori. The rate of loss always increases when stochastic effects are taken into account.

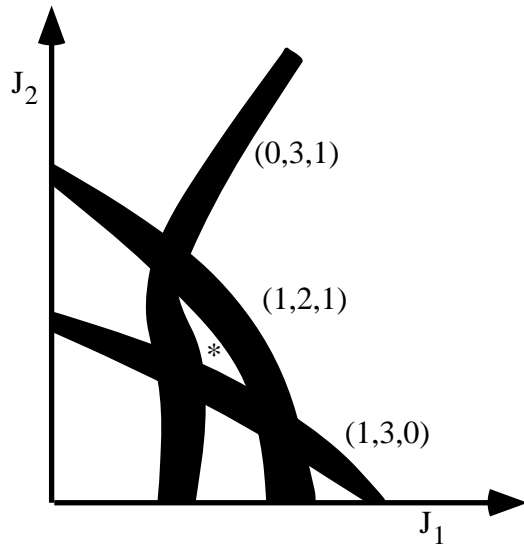


FIG. 1. Resonances of varying width in action space. The asterisk indicates where a KAM surface might be.

B. Fixed points for perturbed four-dimensional maps

The fixed points can be described in terms of either the Hamiltonian or the map. Indeed, both approaches are used here. Since only maps are used in numerical studies, the map approach is given more weight. Because this map is symplectic, it can be described in terms of a mixed-variable generating function, $\varepsilon F(\bar{\theta}, \mathbf{J})$, which is a function of the initial actions \mathbf{J} and the final angles $\bar{\theta}$. The map has the form

$$\bar{\theta}_i = \theta_i + 2\pi\nu_i(\mathbf{J}) + \varepsilon \frac{\partial F}{\partial J_i}(\bar{\theta}, \mathbf{J}) \quad (4)$$

and

$$\bar{\mathbf{J}}_i = \mathbf{J}_i + \varepsilon \frac{\partial F}{\partial \bar{\theta}_i}(\bar{\theta}, \mathbf{J}). \quad (5)$$

This map can be calculated from the Hamiltonian via perturbation theory.

A fixed point of order L is a point that maps onto itself after L iterations of the map. To lowest order, Eq. (4) implies that the unperturbed tunes at the fixed point must satisfy

$$\nu_i = M_i/L, \quad (6)$$

where M_i is an integer between 1 and L . In fact, this is true for the exact map also, at least in the sense of the averaged tunes, because the phase space point comes back to the starting point after L turns. Thus, the tunes are rational at a fixed point, and so they satisfy at least two relations of the form

$$l_1^i \nu_1(\mathbf{J}) + l_2^i \nu_2(\mathbf{J}) - m^i = 0 \quad (i = 1, 2), \quad (7)$$

which are linearly independent. Equations (7) can be solved for the tune since

$$l \equiv l_1^1 l_2^2 - l_2^1 l_1^2 \quad (8)$$

does not vanish. The results are

$$\nu_1 = (l_2^2 m^1 - l_2^1 m^2)/l \quad (9)$$

and

$$\nu_2 = (l_1^1 m^2 - l_1^2 m^1)/l. \quad (10)$$

In general, one does not have $L = l$. Because a fixed point of order L is also a fixed point of order $2L, 3L$, etc., L is taken to be the smallest possible period for the fixed point. This implies that $l_2^2 m^1 - l_2^1 m^2$, $l_1^1 m^2 - l_1^2 m^1$, and L have no common divisor other than unity. Similarly, for any resonance, the common divisors are removed; i.e., it is assumed that neither of the triplets (l_1^i, l_2^i, m^i) has a common divisor. Nevertheless, it is possible that the forms (9) and (10) are not reduced, and so $L \neq l$. An example is that of the two triplets $(9, 12, 2)$ and $(3, 6, 1)$ for which Eq. (8) gives $l = 18$, yet $\nu_1 = 0$ and $\nu_2 = 1/6$.

The relations (8)–(10) give the rational values of the tunes for the fixed points corresponding to the crossing of two resonances. It is not possible to derive an inverse relation as, for any two rational values of the tunes, it is possible to have many different corresponding pairs of resonance: through any one point there may pass more than two lines in tune space corresponding to a relation of the form (3).

The conditions derived thus far specify only the actions (and these only to lowest order), not the angles of fixed points. To obtain the fixed-point angles through lowest order, we assume that the solutions for the fixed points are analytic in the perturbation parameter and can be written as the series

$$J_i^L = J_i^{L,0} + \varepsilon J_i^{L,1} + \dots \quad (11)$$

and

$$\theta_i^L = \theta_i^{L,0} + \varepsilon \theta_i^{L,1} + \dots \quad (12)$$

Inserting these series into Eq. (5) then gives the equations

$$\frac{\partial W}{\partial \theta_i}(\theta^{L,0}) = 0, \quad (13)$$

where

$$W(\theta) \equiv \sum_{k=1}^L F(\theta_i + 2\pi k M_i/L, \mathbf{J}^{L,0}), \quad (14)$$

for the fixed-point angle to lowest order.

There are at least four solutions to Eqs. (13). The function W , being periodic in θ_1 , has a maximum and a minimum for each value of θ_2 . This defines two curves along which $\partial W/\partial \theta_1$ vanishes. Along each of these curves there is a maximum and a minimum. Hence, along each of these curves there are two points at which $\partial W/\partial \theta_2$ vanishes. For N degrees of freedom, this generalizes to there being at least $2N$ solutions to Eqs. (13). Thus, a nearly integrable Hamiltonian has at least $2N$ fixed points at each

rational surface. (This was shown without the use of perturbation theory for reversible maps in Ref. [58].) Furthermore, through a couple of canonical transformation, it can be shown that a Hamiltonian with only two crossing resonances present has exactly $4l$ fixed points of order L .

Inserting these lowest-order results for the angle of the fixed point into Eq. (4) and expanding the tune through first order in the action difference while keeping the action at its unperturbed value in F determines the corrections to the fixed-point action. We will pursue this calculation further, as we have obtained our goal—showing that the fixed points exist to lowest order. Provided the perturbation is sufficiently small, one can then show that the series for the fixed point converges. Hence, fixed points arise at the intersections of resonances, which correspond to rational tunes.

C. Motion near fixed points

The linear stability of fixed points of four-dimensional symplectic maps has been studied extensively by Howard and MacKay [59]. Let $\mathcal{M}(z)$ denote the transfer map of one period of the Hamiltonian, which corresponds to one turn in a circular accelerator. An L th order fixed point of this map satisfies the equation

$$z = \mathcal{M}^L(z) \equiv \mathcal{M}(\mathcal{M}(\mathcal{M}(\dots \mathcal{M}(z)\dots))). \quad (15)$$

The linearized motion near an L th order fixed point is governed by the tangent map T^L , defined as

$$\delta \bar{z} = T^L \cdot \delta z. \quad (16)$$

It is the derivative of the L -times composed map, which can be obtained from

$$\begin{aligned} T_{i,j}^L &= \frac{\partial \mathcal{M}_i^L}{\partial z_j} \\ &= \frac{\partial \mathcal{M}_i}{\partial z_{k_{L-1}}} (\mathcal{M}^{L-1}(z)) \frac{\partial \mathcal{M}_{k_{L-1}}}{\partial z_{k_{L-2}}} (\mathcal{M}^{L-2}(z)) \\ &\quad \times \dots \frac{\partial \mathcal{M}_{k_1}}{\partial z_j} (z). \end{aligned} \quad (17)$$

Because of the symplecticity of the original map, by definition the tangent map T^L is a symplectic matrix. The linear stability is determined by the eigenvalues of this matrix. For symplectic matrices, if λ is an eigenvalue, so are $1/\lambda$, λ^* , and $1/\lambda^*$. Thus, eigenvalues come in complex conjugate pairs on the unit circle ($\lambda = 1/\lambda^*$), inverse pairs on the real line ($\lambda = \lambda$), or complex quadruplets in other parts of the complex plane (see Fig. 2).

The eigenvalues can be found first defining the stability index [60],

$$\rho = \lambda + 1/\lambda \quad (18)$$

for each inverse pair. Given the stability indices, which can be complex, one can solve for the inverse pair of eigenvalues. From the characteristic equation for the polynomial,

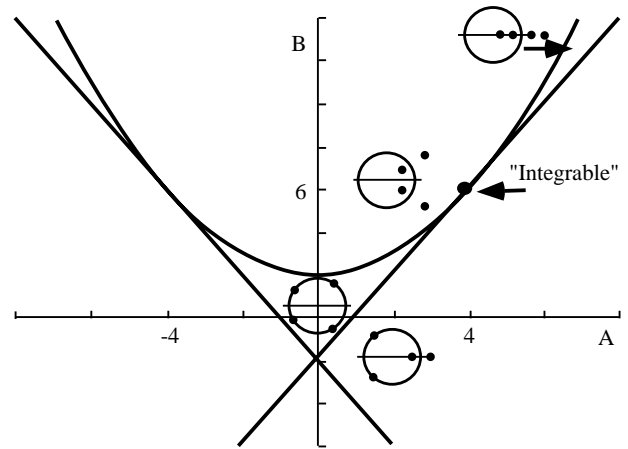


FIG. 2. Linear stability diagram for 4D symplectic maps.

it follows that, the stability indices are the roots of a polynomial,

$$Q(\rho) = \rho^2 - A\rho + B - 2 = 0, \quad (19)$$

where

$$A \equiv \text{Tr}(T) \quad (20)$$

and

$$B \equiv \{[\text{Tr}(T)]^2 - \text{Tr}(T^2)\}/2. \quad (21)$$

It is straightforward to show [61] that, in case of two-dimensional maps, the island width goes to zero, i.e., the resonance vanishes, when the fractional tune of the fixed points vanish, i.e., the eigenvalues of the tangent matrix T are unity. For 4D maps, the picture is qualitatively more complicated, since there are, in principle, an infinite number of resonances intersecting at any given fixed point. It is clear from Eq. (19) that the values of A and B for the eigenvalues of the tangent matrix T to be unity are

$$A = 4 \quad (22)$$

and

$$B = 6. \quad (23)$$

Around a fixed point where two and only two resonances cross (i.e., only two resonance amplitudes are possibly nonzero), we can show that the conditions (22) and (23) guarantee that the amplitudes of those resonances are, in fact, zero. The Hamiltonian near the fixed point is

$$\begin{aligned} H &= H_0(J_1, J_2) + \varepsilon_1 \cos(l_1^1 \theta_1 + l_2^1 \theta_2 - m^1 \Omega s) \\ &\quad + \varepsilon_2 \cos(l_1^2 \theta_1 + l_2^2 \theta_2 - m^2 \Omega s), \end{aligned} \quad (24)$$

where

$$l_1^1 l_2^2 - l_2^1 l_1^2 \neq 0 \quad (25)$$

and

$$H_0 \equiv \nu_1 J_1 + \nu_2 J_2 + \frac{1}{2} \alpha_0 J_1^2 + \beta_0 J_1 J_2 + \frac{1}{2} \gamma_0 J_2^2. \quad (26)$$

After the canonical transformation,

$$\varphi_1 = l_1^1 \theta_1 + l_2^1 \theta_2 - m^1 \Omega s, \quad (27)$$

$$\varphi_2 = l_1^2 \theta_1 + l_2^2 \theta_2 - m^2 \Omega s, \quad (28)$$

$$J_1 = l_1^1 K_1 + l_1^2 K_2, \quad (29)$$

$$J_2 = l_2^1 K_1 + l_2^2 K_2, \quad (30)$$

the Hamiltonian is transformed to

$$\begin{aligned} \mathcal{H} = & \frac{1}{2} \alpha K_1^2 + \beta K_1 K_2 + \frac{1}{2} \gamma K_2^2 + \varepsilon_1 \cos(\varphi_1) \\ & + \varepsilon_2 \cos(\varphi_2). \end{aligned} \quad (31)$$

Linearizing the equations of motion generated from (31) near a stable fixed point, we obtain

$$\ddot{\varphi}_1 + \alpha \varepsilon_1 \varphi_1 + \beta \varepsilon_2 \varphi_2 = 0, \quad (32)$$

$$\ddot{\varphi}_2 + \beta \varepsilon_1 \varphi_1 + \gamma \varepsilon_2 \varphi_2 = 0, \quad (33)$$

from which island tunes can be solved for. The results are

$$\omega_1^2 + \omega_2^2 = \alpha \varepsilon_1 + \gamma \varepsilon_2, \quad (34)$$

$$\omega_1^2 \omega_2^2 = (\alpha \gamma - \beta^2) \varepsilon_1 \varepsilon_2, \quad (35)$$

which imply that $\omega_1 = \omega_2 = 0$ when $\varepsilon_1 = \varepsilon_2 = 0$. Since $\omega_1 = \omega_2 = 0$ means that the eigenvalues of T are unity, we conclude that the resonance driving terms vanish when $A = 4$ and $B = 6$.

The statement above can be generalized one step further. Since a fixed point of order L is also that of order nL , where n is a positive integer, it is also the intersection of resonances (nl_1^1, nl_2^1, nm^1) and (nl_1^2, nl_2^2, nm^2) . When all these resonances are included, the Hamiltonian near the fixed point can be written as

$$\begin{aligned} H = & H_0(J_1, J_2) + g_1(J_1, J_2, l_1^1 \theta_1 + l_2^1 \theta_2 - m^1 \Omega s) \\ & + g_2(J_1, J_2, l_1^2 \theta_1 + l_2^2 \theta_2 - m^2 \Omega s). \end{aligned} \quad (36)$$

After the same transformation, the new Hamiltonian takes the form

$$\begin{aligned} \mathcal{H} = & \frac{1}{2} \alpha K_1^2 + \beta K_1 K_2 + \frac{1}{2} \gamma K_2^2 + G_1(K_1, K_2, \varphi_1) \\ & + G_2(K_1, K_2, \varphi_2), \end{aligned} \quad (37)$$

which can be linearized and becomes

$$\begin{aligned} \mathcal{H} = & \frac{1}{2} \alpha K_1^2 + \beta K_1 K_2 + \frac{1}{2} \gamma K_2^2 \\ & + \frac{\partial^2 G_1}{\partial \varphi_1^2} \varphi_1^2 + \frac{\partial^2 G_2}{\partial \varphi_2^2} \varphi_2^2. \end{aligned} \quad (38)$$

Note that the first derivatives $\partial G_{1,2}/\partial \varphi_{1,2}$ vanish at the fixed point. The equations of motion are the same as those above when $\varepsilon_{1,2}$ are replaced with $\partial^2 G_{1,2}/\partial \varphi_{1,2}^2$. Again, we conclude that the resonance driving terms vanish when $A = 4$ and $B = 6$, provided that the second angular derivatives of the perturbation do not vanish at resonance. We expect that the imposition of this condition leads to an ac-

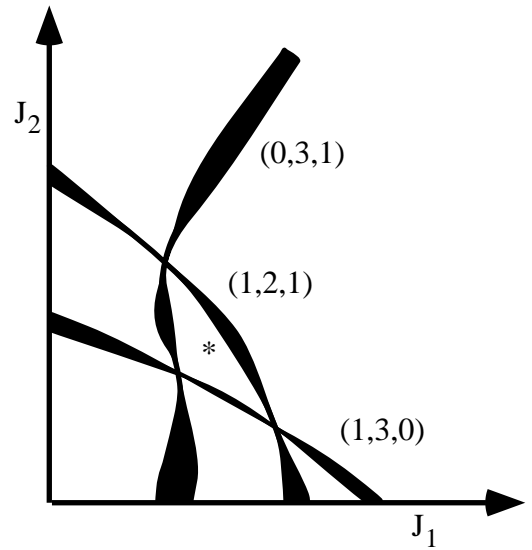


FIG. 3. Action plane showing resonance widths after obtaining $A = 4$ and $B = 6$ at the intersection of the resonance lines so that the resonance widths vanish there.

tion plane as shown in Fig. 3, where the resonance widths are squeezed at the resonance crossings.

When three or more linearly independent resonances intersect at a fixed point, the above argument breaks down. However, if there are three or more comparably sized resonances, it is likely that there are more independent fixed points, and so one has more conditions to impose. For present purposes, further development along this line is not needed, as we will ultimately show through computation that imposition of the conditions, $A = 4$ and $B = 6$, leads to improvement of the dynamic aperture.

D. Resonance correction through adjusting island tunes

Our analysis leads us to a method for enlarging the nearly integrable region of phase space. The fixed points corresponding to the relevant resonance pairs are found. The parameters of the Hamiltonian are varied so as to solve for the values at which the fixed-point parameters satisfy Eqs. (22) and (23). We now turn to a discussion of how this can be carried out to enlarge the nearly integrable region of a given accelerator lattice.

As discussed in Sec. I, perturbations of all kinds make accelerators nonintegrable. Experience in numerical tracking shows that the nearly integrable region is always bounded by a small number of dominant resonances. In case of two-dimensional maps, there is generally only one such resonance [52,62]. Hence, it is necessary to correct them first and try to deal with other weaker resonances later. Until now, however, it has been sufficient to enlarge the nearly integrable region of both two- [52] and four-dimensional (Sec. III) maps by correcting only the dominant resonances. A possible explanation may be that the higher-order resonances are primarily due to nonlinear

beats of the lower-order dominant resonances and, as a result, the higher-order fixed point residues decrease with those of the low-order fixed points.

Specifically, magnetic multipoles are used and their strengths and, in principle, locations are varied to solve for parameter values for which Eqs. (22) and (23) are satisfied for the design energy; i.e.,

$$A_j(\delta \equiv \Delta E/E_0 = 0) - 4 = 0 \quad (39)$$

and

$$B_j(\delta \equiv \Delta E/E_0 = 0) - 6 = 0 \quad (40)$$

are satisfied for fixed-point j related to the dominant resonance(s). In this case we say that our *parameters* are the multipole strengths and, in principle, locations, while the *residuals*, the quantities we want to vanish, are the left-hand sides of Eqs. (39) and (40).

Our procedure for chaos reduction will need to be augmented to provide for a stable range of energies, because the above procedure may lead to lattices for which slightly off-energy particles see large islands and chaotic regions. To prevent this, one could add to the list of the residuals the quantities

$$R_{Ajn} \equiv A_j(\delta_n) - 4 \quad (41)$$

and

$$R_{Bjn} \equiv B_j(\delta_n) - 6, \quad (42)$$

where the offsets δ_n are chosen in the range of desired stable energies. Alternatively, if only a small stable energy interval is needed, one could, in the spirit of conventional lattice design, require the vanishing of the A chromaticity,

$$\chi_{Ajn} \equiv \frac{dA_j}{d\delta}, \quad (43)$$

and the B chromaticity,

$$\chi_{Bjn} \equiv \frac{dB_j}{d\delta}. \quad (44)$$

(These chromaticities are not the usual chromaticities, but they can be related to them.)

In the works of both Ref. [52] and the present article, it was found that one additional residual has to be added to the list, that of the location of the fixed points. Without such a restriction, the variation of parameters can result in the movement of the fixed point toward the origin, where nonlinearity is small (the nonlinear tune shift increases). This can actually result in a decrease in dynamic aperture, as the more distant fixed points, which move inward and determine the dynamic aperture, have not been optimized.

In the implementation of this method it is necessary to be able to find high-order fixed points of four-dimensional maps. This can be difficult because it is much harder to make a good guess of the fixed points comparing to the two-dimensional maps. The difficulty is reduced when one is analyzing maps having inversion symmetry [58],

so that one knows that the odd-order fixed points must lie on a plane. Nonetheless, currently one has to rely heavily on sophisticated numerical optimization software even for maps with inversion symmetry. In the present work, the optimization software package LMDIF [63] is used for both finding fixed points and minimizing the residuals. In general, an optimization package can be used to find the roots of a function $f(x)$ by using it to minimize $[f(x)]^2$.

In fact, there are always many resonances crossing at a given intersection. While higher-order resonances are generally much weaker and can be ignored, resonances of the same order have to be dealt with altogether. To our knowledge, not much is known about the relation between the A and B coefficients and the resonance driving terms when greater than two resonances of the same order cross. But, as demonstrated by the example below, for nearly integrable systems, the difficulty can be overcome by correcting some of the resonances through their crossings with other resonances. By doing so, an implicit assumption is made that, if a resonance is corrected at any point, its width remains small over a sufficiently large interval of the resonance line.

III. THE ADVANCED LIGHT SOURCE (ALS): AN EXAMPLE

An example of numerical study is presented to demonstrate how this method is implemented. Before going into the details specific to the example, a few issues related to the generics of the implementation are discussed.

The general procedure to apply this method is to, first, find the tunes at the edge of the dynamic aperture in order to determine the dominant resonances. Second, the stable fixed points of the intersections of the resonances are selected, found, and the linear transfer matrices around them calculated. Third, the strengths of the correction multipoles are chosen such that Eqs. (39), (40), (43), and (44) are satisfied. Furthermore, in order to keep amplitude dependent tune shift (detuning) constant or to reduce it, the locations of some of the fixed points have to be fixed (*fixed point pinning*). In reality, the second and third steps are repeated and a solution is found iteratively. Finally, the dynamic aperture of the modified lattice is found through tracking study and comparison is made against that of the original lattice.

As in the work of Ref. [52], the method is applied to the Advanced Light Source (ALS) [64]. The obvious reason is the ease of comparison with the previous work. The more compelling motivation is that increasing dynamic aperture is of practical importance to the performance of the Advanced Light Source. It will increase injection efficiency and beam lifetime [65,66]. The ALS ring has 12 identical superperiods, each of which contains three bending magnets, six quadrupoles for focusing, and four sextupoles for chromaticity correction. The superperiod is symmetric about its center. Octupoles are added and their strengths

are used as parameters to reduce chaos and increase dynamic aperture. Because of the fact that the purpose of the work is to assess, in principle, the validity of the new method, the locations of the octupoles were chosen without regard to the physical constraint of the real machine. To make the optimization simple, the A and B chromaticities [Eqs. (43) and (44)] are dropped from the residual list. As shown below, for this example, the A and B chromaticities are not important (see Tables III and IV). But this may not be true for other cases.

Two computer code packages are used in the study. An accelerator tracking code MAPA [67] is used to do the tracking needed. The built-in graphical user interface and the object-oriented nature make it easy to use and modify. COSY INFINITY [68] is chosen to carry out the optimization due to the flexibility of its fitting procedure and the optimization package LMDIF [63] contained in it, which we used to locate fixed points.

Before optimization starts, the dominant resonances must be found. This was done through tracking of the original ALS lattice. Tracking was done element by element, where drifts, dipoles, and quadrupole are represented by a linear matrix and the sextupoles by a kick. Because of the 12-fold symmetry, only one superperiod is used throughout the study. Hence the tunes refer to those of a superperiod. Results show that the tunes at the edge of the dynamic aperture are $\mu_x = 7/6$ and $\mu_y = 2/3$, both of which decrease from the central tunes ($\mu_x = 1.189$, $\mu_y = 0.682$). The values of the tunes imply that four resonances of orders of 6 or lower can be excited, which are

$$\begin{aligned} 6\nu_x &= 7, \\ 3\nu_y &= 2, \\ 2\nu_x + \nu_y &= 4, \\ 2\nu_x + 4\nu_y &= 5. \end{aligned}$$

The crossing of four resonances at one point of the tune (action) plane presents the type of difficulty discussed above. Since there are only two independent variables determining the eigenvalues of the tangent matrix, fitting one set of them to the values of local integrability does not guarantee that all four driving terms vanish. As a result, more independent fixed points have to be used to minimize all the resonances. Besides the four-dimensional sixth-order fixed points at $(7/6, 2/3)$ on the tune plane, a two-dimensional ($y = p_y = 0$) sixth-order fixed point at $(7/6, 0.682)$ and a four-dimensional third-order fixed point at $(7/6, 1)$ are added to the residual list (see Fig. 4). The additional fixed points are responsible for correcting resonances $6\nu_x = 7$ and $3\nu_y = 2$. Experience showed that one more fixed point from each of the points $(7/6, 2/3)$ and $(7/6, 1)$ is needed to obtain a solution. It seems that the two fixed points behave independently when the motion is far from local integrability but are highly correlated when the motion is close to local integrability.

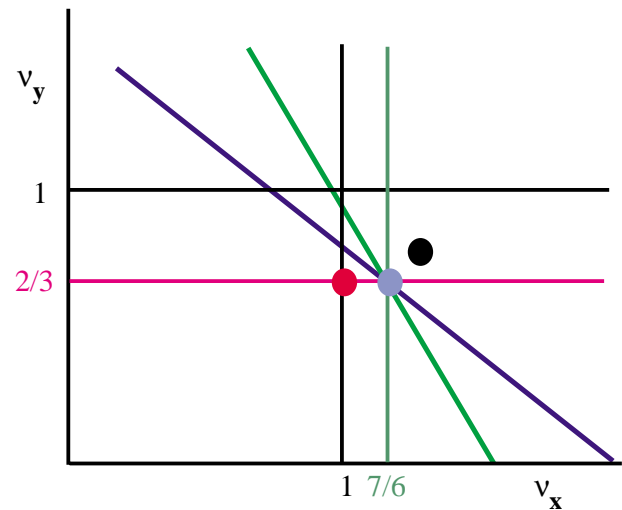


FIG. 4. (Color) Resonance lines in tune space.

Now there are nine members on the residual list. In order to leave room for fixing the location of fixed points (fixed point pinning), 12 instead of nine octupoles are added to the first half of the original superperiod. Therefore, there are 24 octupoles placed in a superperiod so that the mirror symmetry is preserved. The location of the octupoles is shown in Fig. 5.

Similar to tracking, the linear matrix T around a fixed point is obtained through multiplying the matrix of every element. Note that, for drifts, dipoles and quadrupoles, the matrices are the same as the those around the reference orbit because these elements are linear in the model. For sextupoles and octupoles, on the other hand, the matrices depend on the position of the orbit, due to feed-down effect.

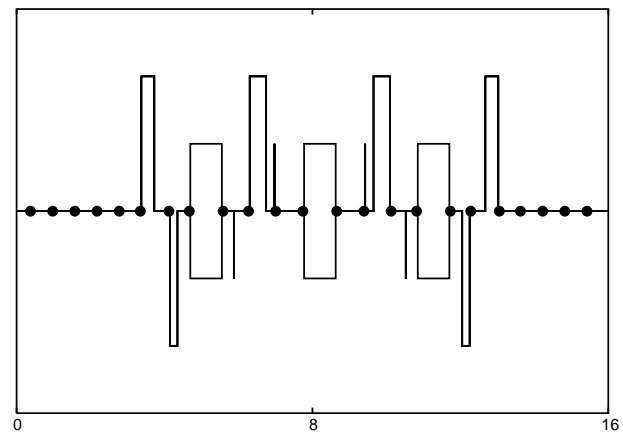


FIG. 5. Layout of a superperiod of the ALS with the additional octupoles. The horizontal axis denotes the length of the reference particle in meters. The rectangles straddling the horizontal axis denote the bends, those above or below the axis are the focussing quads, and the vertical lines denote the sextupoles. The solid dots denote the added octupoles.

TABLE I. Fixed points used and results of their residues: first solution.

	Old A	Old B	New A	New B
2D sixth order	4.116
4D sixth order	3.915	5.806	4.000 08	5.999 96
4D sixth order	3.775	5.580	4.000 08	5.999 96
4D third order	0.028	-2.08	3.999 999 997	5.999 999 998
4D third order	-0.098	-2.05	3.999 999 97	6.000 000 01

At the beginning of the optimization, one fixed point is always pinned to prevent other fixed points from moving towards the origin. To achieve this, the pinned fixed point has to be the one that causes the others to move outward, which is found empirically. With the pinned fixed point selected, optimization proceeds with trying different starting octupole strengths. A solution was found with moderate increase in dynamic aperture (20%). The pole tip field strengths of all octupoles are below 7 kG assuming that their length is 10 cm and the half gap is 5 cm. The A and B values of the fixed points are shown in Table I.

The two-dimensional sixth-order fixed point simply disappeared in the new system due to the fact that $\nu_x(\mathbf{J})$ now increases from the central tune. Instead of decreasing to $7/6$ from 1.189, ν_x in the new system increases to $6/5$ at the edge of the stable region. Since ν_x does not cross $7/6$ anymore, these sixth-order fixed points cease to exist. As a result, the optimizer finds the origin, because the optimization was done in a way that the fixed points and the residues are fitted together.

Our tracking simulations consisted of following an ensemble of particles through the lattice and keeping track of which particles were lost (went to large values of transverse coordinate) within a specified number of turns. (For this intermediate solution, we chose to integrate only 64 turns. We did lengthier runs on the final solution.) To determine the volume of the stable part of the four-dimensional phase space, we choose the ensemble to have initial values evenly spaced in the 4D (x, y, p_x, p_y) phase space. Counting the particles that do not stray far from the

TABLE II. Volume of stable four-dimensional phase space after 64 turns: first solution.

δ	Old [10^{-8} (m rad) 2]	New [10^{-8} (m rad) 2]	Change
-0.005	1.5	3.7	+147%
0.000	1.6	3.1	+94%
0.005	1.8	3.1	+76%

TABLE III. Dynamic aperture after 12 921 turns: first solution.

δ	Old (cm)	New (cm)	Change
-0.005	1.61 ± 0.47	2.17 ± 0.67	+35%
0.000	1.64 ± 0.46	1.80 ± 0.45	+9.8%
0.005	1.64 ± 0.47	1.97 ± 0.34	+20%

initial conditions gives a Monte Carlo evaluation of the integral of the 4D volume of well-confined trajectories. Table II shows the results for the first solution. This table shows that the volume of stable four-dimensional phase space roughly doubles over a wide range of energy after this first correction.

To determine the dynamic aperture, we choose the ensemble to have initial conditions evenly spaced in the x - y plane and to have vanishing initial values of the momenta. Thus, we obtain a Monte Carlo evaluation of the integral of the region of the x - y plane of well-confined trajectories. The equivalent radius, $(A/\pi)^{1/2}$, of this area is the usual dynamic aperture. Table III shows that, for this first solution, the dynamic aperture is increased by 18% over a wide range of energy. This solution did not minimize the A and B chromaticities, thus indicating that at least in some cases the minimization of the A and B chromaticities is not necessary.

The reason for the relatively small amount of increase in dynamic aperture of the solution above is that the dynamic aperture of the horizontal motion decreases from 2.21 to 1.66 cm. Therefore, the solution is to find a way to increase the dynamic aperture of motion in both planes simultaneously. This was done by moving the fixed points farther away from the origin. Roughly speaking, it consisted of different stages during each of which a different fixed point was moved outwards and then pinned. This was necessary because moving and pinning any given fixed point can push

TABLE IV. Fixed points used and results of their residues: final solution.

	Old A	Old B	New A	New B
2D sixth order	4.116
4D sixth order	3.915	5.806	4.087	6.174
4D sixth order	3.775	5.580	4.027	5.986
4D third order	0.028	-2.08	3.999	6.000
4D third order	-0.098	-2.05	3.988	6.002

TABLE V. Volume of stable four-dimensional phase space after 64 turns: final solution.

δ	Old [10^{-8} (m rad) 2]	New [10^{-8} (m rad) 2]	Change
-0.005	1.5	6.4	+327%
0.000	1.6	5.9	+269%
0.005	1.8	5.8	+222%

TABLE VI. Dynamic aperture after 12921 turns: final solution.

δ	Old (cm)	New (cm)	Change
-0.005	1.61 ± 0.47	2.45 ± 0.52	+52%
0.000	1.64 ± 0.46	2.49 ± 0.49	+52%
0.005	1.64 ± 0.47	2.41 ± 0.44	+47%

TABLE VII. The strengths of the octupoles of the final solution. The octupoles are labeled from the starting point of the superperiod to the center (see Fig. 5). The strength is defined as $\frac{1}{6} \frac{d^3 B}{dr^3} s$, where s is the length.

Octupole	Strength ($1/m^3$)	Octupole	Strength ($1/m^3$)
1	-0.8705	7	11.16
2	-9.749	8	-23.93
3	-18.24	9	54.51
4	-49.99	10	-62.03
5	1.388	11	97.07
6	57.67	12	3.602

the others out only to a certain extent. Here the location of the fixed points becomes a convenient measure of detuning. This method was proven to be successful. A final solution was found with a quadrupled volume of stable phase space and a 50% increase of the dynamic aperture over the same range of energy (Tables IV–VI). Similar to the first solution, the octupole strengths are all below 3.5 kG.

The strengths of the octupoles are shown in Table VII. This table shows that most of the octupoles have strengths of the order of tens of $1/m^3$. However, there are three octupoles with strengths less than $5 m^{-3}$. It is possible that these could be eliminated. However, we are leaving sensitivity studies to future work.

IV. CONCLUSIONS AND FUTURE DIRECTIONS

A method for finding four-dimensional symplectic maps with enlarged nearly integrable region is presented and its implementation and validity demonstrated by an example. This method allows one to increase the dynamic aperture to capture (at injection) more particles or to provide a greater volume of stable orbits so that scattering is less likely to cause particle loss. As a result, large dynamic apertures may be achievable in strongly nonlinear machines such as synchrotron light sources, allowing them to produce light beams of greater brightness (see Ref. [69] for a different approach).

Future work includes research oriented towards reducing the number of required magnets. One direction is to carry out sensitivity studies; another is to experiment with different types of multipoles. Octupoles were chosen because they affect the nonlinear tune in first order without modifying the linear tune or the chromaticity. However, they cause large fixed point movements because of their modifications of the nonlinear tune. Future work could include

trying multiple sextupoles, chosen so that their integrated effect on chromaticity vanishes or put in dispersion free regions. Additionally, decupoles might be used as they have the greatest effect at the larger deviations from the design orbit, at the dynamic aperture limit, while at the same time having no affect on the nonlinear tune in first order. Finally, we note that the position as well as the strength of the multipoles could be used. This doubles the number of fitting parameters available per multipole.

ACKNOWLEDGMENTS

The authors gratefully acknowledge helpful conversations with Dr. S. G. Shasharina and Dr. K. Oide. This work was supported by the U.S. Department of Energy under Grant No. DE-FG03-95ER40926.

- [1] H. Poincaré, *Les Methodes Nouvelles de la Mecanique* (Gauthier-Villars, Paris, 1893), Vol. 2.
- [2] C. L. Siegel, *Ann. Math.* **42**, 806 (1941).
- [3] A. N. Kolmogorov, *Dokl. Akad. Nauk. SSSR* **98**, 527 (1954).
- [4] V. I. Arnold, *Dokl. Akad. Nauk. SSSR* **138**, 13 (1961) [*Sov. Math. Dokl.* **2**, 501 (1961)].
- [5] J. Moser, *Nachr. Akad. Wiss. Goett. Ila, Math.-Phys. Kl.* **1**, 1 (1962).
- [6] V. I. Arnold and A. Avez, *Ergodic Problems of Classical Mechanics* (Addison-Wesley, Redwood City, CA, 1989).
- [7] V. K. Melnikov, *Trans. Moscow Math. Soc.* **12**, 1 (1963).
- [8] P. J. Holmes and J. E. Marsden, *J. Math. Phys. (N.Y.)* **23**, 669 (1982).
- [9] J. Moser, *Nachr. Akad. Wiss. Goett. Ila, Math.-Phys. Kl.* **6**, 87 (1955).
- [10] R. Hagedorn, CERN Report No. 57-1, 1957.
- [11] A. Schoch, CERN Report No. 57-21, 1958, and references therein.
- [12] P. A. Sturrock, *Ann. Phys. (N.Y.)* **3**, 113 (1958).
- [13] H. Meier and K. R. Symon, in *Proceedings of the International Conference on High Energy Accelerators, Geneva* (CERN, Geneva, 1959), p. 253.
- [14] S. Ohnuma and R. L. Gluckstern, *IEEE Trans. Nucl. Sci.* **22**, 1851 (1976).
- [15] G. Guignard, CERN Report No. 78-11, 1978.
- [16] F. Willeke, Fermilab Report No. FN-422, 1985.
- [17] D. Neuffer, *Part. Accel.* **23**, 22 (1988).
- [18] E. Forest, M. Berz, and J. Irwin, *Part. Accel.* **24**, 91 (1989).
- [19] M. Berz, in *Proceedings of the International Workshop on Nonlinear Problems in Accelerator Physics*, IOP Conf. Proc. No. 131 (Institute of Physics and Physical Society, London, 1993), p. 77.
- [20] P. Zhang and S. Machida, in *Proceedings of the 1993 Particle Accelerator Conference, Washington, DC* (IEEE, Piscataway, NJ, 1993), p. 176.
- [21] J. Laskar and D. Robin, *Part. Accel.* **54**, 183 (1996).
- [22] A. Bazzani *et al.*, CERN Report No. 94-02, 1994.
- [23] U. Wienands and X. Wu, in *The SSC Low Energy Booster* (IEEE, New York, 1997), p. 22.
- [24] R. Bartolini and F. Schmidt, *Part. Accel.* **59**, 93 (1998).

- [25] Y. Papaphilippou and F. Schmidt, in *Nonlinear and Collective Phenomena in Beam Physics*, edited by S. Chattopadhyay, AIP Conf. Proc. No. 468 (AIP, New York, 1999), p. 107.
- [26] A. Verdier, in *Proceedings of the Particle Accelerator Conference, New York, 1999* (IEEE, Piscataway, NJ, 1999), p. 398.
- [27] F. Schmidt and A. Verdier, in *Proceedings of the Particle Accelerator Conference, New York, 1999* (Ref. [26]), p. 1563.
- [28] J. Wei *et al.*, in *Proceedings of the Particle Accelerator Conference, New York, 1999* (Ref. [26]), p. 2921.
- [29] T. Sen, N. Gelfand, and W. Wan, Fermilab Report No. FERMILAB-Conf-99/276, 1999.
- [30] R.T. Burgess and J.M. Jowett, CERN Report No. CERN-SL-2000-025, 2000.
- [31] E.D. Courant, in *Proceedings of the International Conference on High Energy Accelerators, Geneva* (CERN, Geneva, 1956), p. 254.
- [32] M. Barbier and A. Schoch, CERN Report No. 58-5, 1958.
- [33] R. Steining and E.J.N. Wilson, Nucl. Instrum. Methods **121**, 275 (1974).
- [34] J.P. Gourber, CERN Report No. ISR-MA/74-54, 1974.
- [35] K.H. Schindl, IEEE Trans. Nucl. Sci. **26**, 3562 (1979).
- [36] A.W. Chao *et al.*, Phys. Rev. Lett. **61**, 2752 (1988).
- [37] L.R. Evans, in *Frontiers of Particle Beams: Observation, Diagnosis and Correction*, Lecture Notes in Physics Vol. 343 (Springer-Verlag, New York, 1988), p. 209.
- [38] D.A. Edwards and M.J. Syphers, in *Frontiers of Particle Beams: Observation, Diagnosis and Correction* (Ref. [37]), p. 221.
- [39] S.Y. Lee *et al.*, Phys. Rev. Lett. **67**, 3768 (1991).
- [40] P. Zhang, Fermilab Report No. FN-577, 1991.
- [41] J.M. Jowett, in *Proceedings of the 7th LEP Performance Workshop, Chamonix, France, 1997* (CERN Report No. CERN-SL-97-006-DI, 1997), p. 76.
- [42] J.M. Jowett, in *Proceedings of the 8th LEP Performance Workshop, Chamonix, France, 1998* (CERN Report No. CERN-SL-98-006-DI, 1998), p. 85.
- [43] R. Bartolini *et al.*, in *Proceedings of the Particle Accelerator Conference, New York, 1999* (Ref. [26]), p. 1557.
- [44] M. Ball *et al.*, in *Proceedings of the Particle Accelerator Conference* (Ref. [26]), pp. 1545, 1548, and references therein.
- [45] W. Wan, in *Proceedings of the Particle Accelerator Conference, New York, 1999* (Ref. [26]), p. 395.
- [46] J. Wei, ICFA Beam Dynamics Newsletter **21**, 26 (2000).
- [47] A.G. Ruggiero, in *Proceedings of the 9th International Conference on High Energy Accelerators, Stanford, CA, 1974* (U.S. Department of Commerce, Springfield, VA, 1974), p. 265.
- [48] J.R. Cary, Phys. Rev. Lett. **49**, 276 (1982); J.R. Cary, Phys. Fluids **27**, 119 (1984).
- [49] J.D. Hanson and J.R. Cary, Phys. Fluids **27**, 767 (1984); J.R. Cary and J.D. Hanson, Phys. Fluids **29**, 2464 (1986).
- [50] J.R. Cary and R.G. Littlejohn, Ann. Phys. (N.Y.) **151**, 1 (1983).
- [51] B.A. Carreras *et al.*, Nucl. Fusion **28**, 1195 (1988).
- [52] C.C. Chow and J.R. Cary, Phys. Rev. Lett. **72**, 1196 (1994).
- [53] J.R. Cary, Part. Accel. **54**, 151 (1996).
- [54] W. Wan and J.R. Cary, Phys. Rev. Lett. **81**, 3655 (1998).
- [55] J.D. Meiss, Rev. Mod. Phys. **64**, 795 (1992).
- [56] B.V. Chirikov, Phys. Rep. **52**, 265 (1979).
- [57] M. Toda, J. Phys. Soc. Jpn. **22**, 431 (1967).
- [58] H.T. Kook and J.D. Meiss, Physica (Amsterdam) **35D**, 65 (1989).
- [59] J.E. Howard and R.S. MacKay, J. Math. Phys. (N.Y.) **28**, 1036 (1987).
- [60] R. Brouke, AIAA J. **7**, 1003 (1969).
- [61] R.D. Ruth, in *Nonlinear Dynamics Aspects of Particle Accelerators*, Lecture Notes in Physics Vol. 247 (Springer-Verlag, New York, 1986).
- [62] L. Michelotti, *Intermediate Classical Dynamics with Applications to Beam Physics* (Wiley, New York, 1995), Sec. 5.2.3.
- [63] J. Moré, B. Garbow, and K. Hillstrom, Argonne National Laboratory Report No. ANL-80-74, 1980; J. Moré *et al.*, in *Sources and Development of Mathematical Software*, edited by W.R. Cowell (Prentice-Hall, Englewood Cliffs, NJ, 1984).
- [64] A. Jackson, LBNL Report No. LBL-22193, 1987.
- [65] W. Decking, J. Byrd, C. Kim, and D. Robin, in *Proceedings of the 6th European Particle Accelerator Conference, Stockholm, Sweden, 1998* (Institute of Physics, Bristol, UK, 1998), p. 1262.
- [66] W. Decking and D. Robin, in *Proceedings of the Particle Accelerator Conference, New York, 1999* (Ref. [26]), p. 1581.
- [67] S.G. Shasharina, W. Wan, and J.R. Cary, in *Proceedings of the 5th European Particle Accelerator Conference, Barcelona, Spain, 1996* (Institute of Physics, Bristol, UK, 1996), p. 1301.
- [68] M. Berz, Superconducting Cyclotron Laboratory, MSU Technical Report No. MSUCL-977, 1995.
- [69] M. Cornacchia, W.J. Corbett, and K. Halbach, in *Proceedings of the Particle Accelerator Conference, 1991, San Francisco* (SLAC Report No. SLAC-PUB-5528, 1991).